

1 Characterization of carbonaceous aerosols outflow from India and 2 Arabia: Biomass/biofuel burning and fossil fuel combustion

3 S. A. Guazzotti,¹ D. T. Suess,^{1,2} K. R. Coffee,^{1,3} P. K. Quinn,⁴ T. S. Bates,⁴ A. Wisthaler,⁵
4 A. Hansel,⁵ W. P. Ball,⁶ R. R. Dickerson,⁷ C. Neusüß,⁸ P. J. Crutzen,^{9,10} and K. A. Prather¹

5 Received 2 December 2002; revised 25 February 2003; accepted 11 March 2003; published XX Month 2003.

6 [1] A major objective of the Indian Ocean Experiment (INDOEX) involves the
7 characterization of the extent and chemical composition of pollution outflow from the
8 Indian Subcontinent during the winter monsoon. During this season, low-level flow
9 from the continent transports pollutants over the Indian Ocean toward the Intertropical
10 Convergence Zone (ITCZ). Traditional standardized aerosol particle chemical analysis,
11 together with real-time single particle and fast-response gas-phase measurements
12 provided characterization of the sampled aerosol chemical properties. The gas- and
13 particle-phase chemical compositions of encountered air parcels changed according to
14 their geographic origin, which was traced by back trajectory analysis. The temporal
15 evolutions of acetonitrile, a long-lived specific tracer for biomass/biofuel burning,
16 number concentration of submicrometer carbon-containing particles with potassium
17 (indicative of combustion sources), and mass concentration of submicrometer non-sea-
18 salt (nss) potassium are compared. High correlation coefficients ($0.84 < r^2 < 0.92$) are
19 determined for these comparisons indicating that most likely the majority of the species
20 evolve from the same, related, or proximate sources. Aerosol and trace gas
21 measurements provide evidence that emissions from fossil fuel and biomass/biofuel
22 burning are subject to long-range transport, thereby contributing to anthropogenic
23 pollution even in areas downwind of South Asia. Specifically, high concentrations of
24 submicrometer nss potassium, carbon-containing particles with potassium, and
25 acetonitrile are observed in air masses advected from the Indian subcontinent,
26 indicating a strong impact of biomass/biofuel burning in India during the sampling
27 periods (74 (± 9))% biomass/biofuel contribution to submicrometer carbonaceous
28 aerosol). In contrast, lower values for these same species were measured in air masses
29 from the Arabian Peninsula, where dominance of fossil fuel combustion is suggested by
30 results from single-particle analysis and supported by results from gas-phase
31 measurements (63 (± 9))% fossil fuel contribution to submicrometer carbonaceous
32 aerosol). Results presented here demonstrate the importance of simultaneous, detailed
33 gas- and particle-phase measurements of related species when evaluating possible
34 source contributions to aerosols in different regions of the world. *INDEX TERMS:* 0305
35 Atmospheric Composition and Structure: Aerosols and particles (0345, 4801); 0345 Atmospheric
36 Composition and Structure: Pollution—urban and regional (0305); 0394 Atmospheric Composition and
37 Structure: Instruments and techniques; *KEYWORDS:* INDOEX, aerosol chemical characterization, biomass
38 burning, fossil fuel combustion

39 **Citation:** Guazzotti, S. A., et al., Characterization of carbonaceous aerosols outflow from India and Arabia: Biomass/biofuel burning
40 and fossil fuel combustion, *J. Geophys. Res.*, 108(0), XXXX, doi:10.1029/2002JD003277, 2003.

¹Department of Chemistry and Biochemistry, University of California, San Diego, California, USA.

²Now at Department of Chemistry, University of California, Riverside, California, USA.

³Now at Lawrence Livermore National Laboratory, Livermore, California, USA.

⁴Pacific Marine Environmental Laboratory, NOAA, Seattle, Washington, USA.

⁵Institut für Ionenphysik, University of Innsbruck, Innsbruck, Austria.

⁶Department of Chemistry, University of Maryland, College Park, Maryland, USA.

⁷Department of Meteorology and Department of Chemistry, University of Maryland, College Park, Maryland, USA.

⁸Institut für Troposphärenforschung, Leipzig, Germany.

⁹Max-Planck Institute for Chemistry, Mainz, Germany.

¹⁰Also at Scripps Institution of Oceanography, University of California, San Diego, California, USA.

1. Introduction

[2] Anthropogenic activities influence the chemical composition of the atmospheric aerosol, therefore affecting climate, visibility, and human health. Knowledge of the chemical composition and size distribution of aerosol particles, as well as the chemical characteristics and mixing ratios of different species present in the gas phase, is essential for understanding atmospheric processing that affects the composition of aerosols as well as for identification of their sources. During the past few years, increases in the concentration of atmospheric aerosols due to anthropogenic activities have been the focus of many studies [e.g., IPCC, 1996; Schwartz, 1996; Schwartz and Andreae, 1996]. Almost five-fold increases in concentrations of certain species (e.g., nitrates, sulfates) have been indicated for regions downwind of the Indian Subcontinent in the last twenty years [Ball et al., 2003].

[3] Combustion processes such as biomass/biofuel burning and fossil fuel combustion are significant sources of anthropogenic aerosol particles and gases [e.g., Andreae and Crutzen, 1997; Yamasoe et al., 2000; Andreae and Merlet, 2001]. Particles emitted from these sources can affect the radiation balance due to their ability to reflect and absorb solar radiation (direct effect) and act as cloud condensation nuclei, therefore affecting cloud properties (indirect effect) [e.g., Twomey, 1997; Coakley and Cess, 1985; Desalmand et al., 1985; Hallet et al., 1989; Crutzen and Andreae, 1990; Andreae, 1991; Cachier and Ducret, 1991; Charlson et al., 1991; Kuhlbusch et al., 1996; Rosenfeld, 2000]. Emissions from biomass/biofuel burning and other combustion sources which emit black carbon can significantly heat the atmosphere [e.g., Crutzen and Andreae, 1990; Penner et al., 1992, 1993; Haywood and Shine, 1995, 1997; Iversen and Tarrason, 1995; Cooke and Wilson, 1996; Haywood et al., 1997; Haywood and Boucher, 2000; Iversen et al., 1998; Podgorny et al., 2000; Jacobson, 2001; Ramanathan et al., 2001]. Penner et al. [1992] have shown that the direct and indirect effects of smoke aerosols arising from biomass burning could be of comparable significance.

[4] Biomass fuels account for approximately 14% of the world's energy consumption [Hall et al., 1992], with much higher values being reported for developing countries. In India, biomass/biofuel burning (including wood, agricultural residues and dung-cakes used as fuel) is considered to be a major source of energy [Ravindranath and Hall, 1995] and a considerable source of pollution [Hall et al., 1994; Dickerson et al., 2002]. High overall increases in the consumption of petroleum, biofuels, and coal have been reported for the Indian subcontinent. Up to 45% of global emissions of black carbon have been attributed to biomass/biofuel burning [e.g., Kuhlbusch et al., 1996] with emissions from India [1990] estimated to account for 0.45–1 Tg yr⁻¹ [Reddy and Venkataraman, 2000]. Direct observations show that the emissions could be as high as 3 Tg yr⁻¹ [Dickerson et al., 2002].

[5] The Indian Ocean Experiment, INDOEX, was an integrated field campaign which had as a primary goal evaluating the significance of the direct and indirect effects of continental aerosols [Ramanathan et al.,

1995, 1996, 2001; Satheesh et al., 1999; Mitra, 1999]. Characterization of the extent and chemical composition of pollution outflow from the Indian subcontinent and evaluation of the significance of long-range transport of continental aerosols to remote regions in the Indian Ocean were of particular interest [Ramanathan et al., 1995, 1996; 2001]. Ramanathan et al. [2001] have highlighted, from results obtained during the INDOEX campaign, the impact of the Indo-Asian haze on global climate. The biomass/biofuel and fossil fuel contributions to this Indo-Asian haze have been reported to be under debate [UNEP, 2002]. The INDOEX intensive field phase (INDOEX-IFP) was carried out in February and March 1999, during the winter monsoon (NE-monsoon), when low level flow from the continent transports pollutants over the Indian Ocean toward the Intertropical Convergence Zone (ITCZ), where pristine southern hemisphere air masses meet with contrasting polluted continental air masses from the northern hemisphere. During the IFP, the contribution of anthropogenic aerosols to the total loading has been estimated to be as high as 80% over most of the sampled south Asian region and Northern Indian Ocean [Ramanathan et al., 2001].

[6] Several measurements were performed during the campaign on different platforms (for a detailed description see Lelieveld et al. [2001] and Ramanathan et al. [2001]). Results from aerosol particle and gas-phase measurements carried out during leg 2 of the INDOEX cruise on board of the NOAA Research Vessel (R/V) Ronald H. Brown are presented here. Chemical characterization of sampled aerosol particles included mass concentrations of submicrometer non-sea-salt (nss) potassium (K⁺), nss sulfates, black carbon (BC), organic carbon (OC), and number concentration of submicrometer carbon-containing particles with K⁺. In the gas-phase, the volume mixing ratio of acetonitrile (methyl cyanide, CH₃CN) was measured. During the sampling period, the ITCZ was mostly located between the equator and 12°S [Ramanathan et al., 2001; Ball et al., 2003]. Detailed information on the R/V Ronald H. Brown cruise during INDOEX can be found in Ball et al. [2003]. The capability descriptions for this vessel are presented in Parsons and Dickerson [1999].

[7] Acetonitrile is regarded as a relatively long-lived, selective tracer for biomass/biofuel burning [Lobert et al., 1990; Bange and Williams, 2000], predominantly emitted by smoldering biomass fires [Lobert et al., 1990; Holzinger et al., 1999]. In the particle phase, black carbon BC in the submicrometer size range is used as a good general tracer for incomplete combustion from fossil fuel and biomass burning [e.g., Cachier et al., 1989], while nss K⁺ is considered to be a good indicator for biomass/biofuel burning in submicrometer particles [e.g., Andreae, 1983; Cachier et al., 1991; Gaudichet et al., 1995; Andreae et al., 1996]. In particular, the relative contributions from biomass and fossil fuel emissions can be evaluated from the ratio between submicrometer nss K⁺ and BC [Andreae, 1983]. From single particle measurements, submicrometer soot particles containing K⁺ have been indicated as possible tracers for biomass/biofuel burning [Gaudichet et al., 1995]. Single-particle results obtained during INDOEX and combustion

164 source characterization experiments provide an indication of
 165 probable sources of the carbonaceous aerosol.

166 2. Experimental Setup

167 [8] The data presented herein were obtained from 4
 168 March 1999 (Day of Year, DOY 63) until 23 March 1999
 169 (DOY 82) during leg 2 of the NOAA R/V Ronald H. Brown
 170 1999 INDOEX cruise. The cruise started in Male', the
 171 capital of the Republic of the Maldives, proceeding along
 172 the west coast of India and turning south on 11 March
 173 (DOY 70). The southern-most point during leg 2 (13°S) was
 174 reached on 19 March (DOY 78).

175 2.1. Submicrometer Non-Sea-Salt (nss) Potassium 176 and nss Sulfates Mass Concentration

177 [9] Two independent research groups on board the NOAA
 178 R/V Ronald H. Brown, namely NOAA, Pacific Marine
 179 Environmental Laboratory (PMEL), Seattle, Washington
 180 and Department of Meteorology, University of Maryland,
 181 College Park (UMD), measured submicrometer nss K⁺ and
 182 nss sulfate mass concentrations. PMEL used two-stage multi-
 183 jet cascade impactors [Berner et al., 1979] sampling air at
 184 55% RH to determine the submicrometer ($D_{50,aero} < 1.1 \mu\text{m}$)
 185 concentration of sulfates and K⁺. The impaction stage at the
 186 inlet of the impactor was coated with silicone grease to
 187 prevent the bounce of larger particles onto the downstream
 188 stages. A Millipore Fluoropore filter (1.0 μm pore size) was
 189 used for the submicrometer collection substrate. Filters were
 190 wetted with 1 mL of spectral grade methanol. An additional
 191 5 mL aliquot of distilled deionized water was added to the
 192 solution and the substrates were extracted by sonicating for
 193 30 min. The extracts were analyzed by ion chromatography
 194 [Quinn et al., 1998]. Blank levels were determined by
 195 loading an impactor with substrates but not drawing any air
 196 through them. In the case of UMD, two high volume Sierra
 197 impactors, one cascade and one bulk, were used to collect
 198 aerosol samples [Howell et al., 1998]. The cascade impactor
 199 consisted of five stages that segregated the total particular
 200 material into six size fractions. Slotted Whatman 41 filters
 201 were used as the impaction surfaces. The mean aerodynamic
 202 diameter for the stages reported here were 0.74, 0.48, and
 203 0.24 μm [Pszenny, 1992]. A backup filter collected particles
 204 under 0.24 μm . The bulk impactor consisted of a 20 cm by
 205 25 cm Whatman filter. After sampling, filters were placed
 206 into individual polyethylene bags and refrigerated. On alter-
 207 nate days, samples were analyzed on the ship as described by
 208 Quinn et al. [1998]. The remaining samples were analyzed
 209 upon return to the United States using the same method.
 210 Results presented here for UMD correspond to particles
 211 with mean aerodynamic diameters smaller than 0.74 μm .
 212 In both cases, nss K⁺ concentrations were calculated
 213 from Na⁺ concentrations and the ratio of K⁺ to sodium in
 214 seawater. Similarly, nss sulfate concentrations were evalu-
 215 ated from the measured sulfate concentrations and the
 216 corresponding sulfate-to-sodium ratio in seawater.

217 2.2. Black Carbon/Organic Carbon (BC/OC) 218 Mass Concentration

219 [10] Submicrometer particles in the range $0.18 < D_p < 1.1$
 220 μm were collected using a three-stage multijet cascade
 221 impactor [Berner et al., 1979] as described in Neusüß et

al. [2002a]. For the determination of BC/OC, a thermo- 222
 graphic method (Ströhlein C-mat 5500 carbon analyzer) 223
 was operated at a temperature of 590°C to volatilize the OC 224
 fraction within 8 min under nitrogen. The BC fraction of 225
 aerosol particle samples was determined by subsequent 226
 combustion at 650°C in an oxygen atmosphere. For a 227
 detailed explanation of the method used for the evaluation 228
 of BC/OC during the INDOEX cruise, as carried out by the 229
 research group from the Institute for Tropospheric Research, 230
 Germany, refer to Neusüß et al. [2002a]. It is important to 231
 mention that, although there are several methods to deter- 232
 mine separately OC and BC, there is no technique that is 233
 commonly accepted. Methods currently in use include 234
 extraction and thermodesorption methods, with the latter 235
 method having the advantage of being less labor intensive. 236
 Comparison experiments among the different techniques for 237
 BC/OC yield sufficient comparability of total carbon (TC) 238
 values but a wide spread in results of OC and BC determi- 239
 nations. [Cadde and Mulawa, 1990; Countes, 1990; Shah 240
 and Rau, 1991; Schmid et al., 2001]. The method used for 241
 the determination described here typically leads to higher 242
 BC/OC ratios compared to related techniques (i.e., provides 243
 a lower limit for OC and an upper limit for BC), but it has 244
 the advantage of lacking positive artifacts. Quartz fiber filter 245
 sampling for the evaluation of OC show typically high 246
 positive sampling artifacts due to the absorption of volatile 247
 organic species [e.g., Turpin et al., 1994]. Such positive 248
 artifacts are expected to be low for impactor sampling, since 249
 foils have a much smaller surface than the fiber filters. 250
 Better impactor sampling efficiencies, compared to filter 251
 sampling for semivolatile particles, have been observed by 252
 Wang and John [1988] and Neusüß et al. [2002b]. This 253
 might be due to reduced aeration of collected particles on 254
 the impactor substrates compared to filter substrates, possi- 255
 bly over compensating losses due to the pressure drop in the 256
 impactor. However, the low pressure could lead to losses of 257
 semivolatile organic compounds during sampling, mainly 258
 for the submicrometer particle fraction. The method has not 259
 been corrected for any sampling artifacts. 260

261 2.3. Single-Particle Analysis

262 [11] Data on individual particle size and chemical com- 262
 position were obtained by the research group from the 263
 University of California, San Diego using a transportable 264
 aerosol time-of-flight mass spectrometer (ATOFMS) as 265
 described in the literature [e.g., Prather et al., 1994; Noble 266
 and Prather, 1996; Gard et al., 1997]. In these instruments, 267
 the transit times for particles travelling between two scatter- 268
 ing lasers are measured, recorded, and correlated with the 269
 individual particle aerodynamic diameters after proper 270
 instrument calibration. Chemical information for each 271
 detected particle is obtained from positive and negative 272
 ion time-of-flight mass spectra acquired in the instrument, 273
 and correlated with the aerodynamic diameter measured for 274
 each particle. Detected particles are classified into exclusive 275
 chemical categories from the mass spectral information 276
 obtained for each individual particle. Particle number con- 277
 centrations for different particle classes are then evaluated 278
 by carrying out scaling procedures to account for differ- 279
 ences in particle transmission into the ATOFMS [e.g., 280
 Hughes et al., 1999; Allen et al., 2000]. In this particular 281
 case, ATOFMS data were scaled by comparison with 282

283 number concentration data obtained with other shipboard
 284 particle sizing instrumentation (i.e., Optical Particle Counter
 285 (OPC), and a Scanning Mobility Particle Sizer (SMPS))
 286 [Wenzel *et al.*, 2003]. A more detailed explanation on the
 287 instrumental set-up used during the campaign as well as of
 288 the types of particles observed during INDOEX is presented
 289 by Guazzotti *et al.* [2001]. All the single particle results
 290 presented herein correspond to particles with aerodynamic
 291 diameters between 0.3 and 1.0 μm .

292 2.4. Fast-Response Acetonitrile Measurements 293 by PTR-MS

294 [12] Fast-response measurements of acetonitrile were
 295 performed using Proton-Transfer-Reaction Mass Spectrom-
 296 etry (PTR-MS) by the research group from Institut für
 297 Ionenphysik, University of Innsbruck, Austria [Hansel *et al.*,
 298 1995; Lindinger *et al.*, 1998]. PTR-MS is a chemical
 299 ionization mass spectrometry technique based on proton
 300 transfer reactions with H_3O^+ ions for on-line measurements
 301 of organic trace gases in air. PTR-MS measurements during
 302 INDOEX-IFP have been described in detail by Sprung *et al.*
 303 [2001] and Wisthaler *et al.* [2002], thus only the essential
 304 points are outlined here. Ambient air was continuously
 305 sampled through a Teflon[®] PFA tube (length: 50 m; OD:
 306 6.4 mm) from the top of the Ronald H. Brown bow tower
 307 (28 m above sea surface) and led into the PTR-MS instru-
 308 ment. Chemical ionization of acetonitrile (producing the
 309 CH_3CNH^+ ion at mass-to-charge ratio (m/z) 42) was
 310 achieved using proton-transfer-reactions with primary
 311 H_3O^+ ions in a flow drift tube. Primary and product ions
 312 were mass analyzed in a quadrupole mass spectrometer and
 313 detected by a secondary electron multiplier/pulse counting
 314 system. The sensitivity for acetonitrile was calculated fol-
 315 lowing the procedure outlined in detail by Sprung *et al.*
 316 [2001]. The instrumental background was determined by
 317 passing the ambient air through a heated platinum catalyst
 318 (350°C) scrubber. Accuracy for the acetonitrile measure-
 319 ments of $\pm 30\%$ was inferred from intercomparison measure-
 320 ments described by Sprung *et al.* [2001].

321 2.5. Aerosol Absorption Coefficient

322 [13] The absorption coefficients for submicrometer aero-
 323 sol particles were measured at 55% RH by monitoring
 324 the change in transmission through a filter with a Particle
 325 Soot Absorption Photometer (PSAP, Radiance Research).
 326 Measured values were corrected for a scattering artifact,
 327 the deposit spot size, the PSAP flow rate, and the manufacturer's
 328 calibration as per Bond *et al.* [1999]. Values are reported at
 329 0°C , 1013 mbar, and 550 nm. Sources of uncertainty in the
 330 PSAP measurement include noise, drift, correction for the
 331 manufacturer's calibration, and correction for the scattering
 332 artifact [Anderson *et al.*, 1999]. A quadrature sum of these
 333 errors yields absolute uncertainties of 0.38 and 2.8 Mm^{-1}
 334 for absorption coefficients equal to 0.68 and 13 M m^{-1} ,
 335 respectively. These measurements were carried out by
 336 PMEL.

337 3. Results and Discussion

338 3.1. Carbon-Containing Particles With Potassium

339 [14] During INDOEX, the majority of detected particles
 340 with aerodynamic diameters between 0.3 and 1.0 μm were

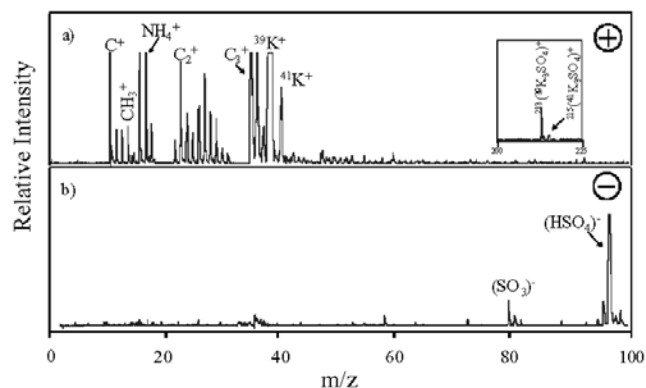


Figure 1. (a) Positive and (b) negative ion mass spectra of a carbon-containing particle with potassium acquired during INDOEX. Peak identifications correspond to the most probable assignments for each particular m/z ratio.

classified as carbon-containing particles by ATOFMS single
 particle analysis [Guazzotti *et al.*, 2001]. Between 20 and
 73% of the submicrometer carbon-containing particles
 detected with the ATOFMS contained K^+ as well, depend-
 ing on the location considered [Guazzotti *et al.*, 2001]. The
 presence of K^+ in submicrometer carbon-containing par-
 ticles has been described to be an indicator of biomass/
 biofuel combustion [e.g., Andreae, 1983; Gaudichet *et al.*,
 1995; Andreae *et al.*, 1996; Andreae and Crutzen, 1997;
 Silva *et al.*, 1999; Yamasoe *et al.*, 2000] and/or coal
 combustion (D. T. Suess *et al.*, manuscript in preparation).
 Potassium is not detected in emissions from light duty
 gasoline powered vehicles currently in use in the U.S.
 (mostly four-stroke engines) [Silva and Prather, 1997].
 Also, submicrometer soot particles emitted from diesel
 engine exhaust have been reported to contain no detectable
 amounts of potassium [Gaudichet *et al.*, 1995]. However,
 no ATOFMS data are available for the vehicle fleet cur-
 rently in use on the Indian Subcontinent (mostly two-stroke
 engines [UNEP, 1999] for which emission data are also
 lacking [Dickerson *et al.*, 2002]).

[15] ATOFMS positive and negative ion mass spectra
 representative of a typical carbon-containing particle with
 K^+ are presented in Figure 1. In the positive ion mass
 spectrum (Figure 1a), C^+ , $(\text{CH}_3)^+$, $(\text{C}_2)^+$, $(\text{C}_2\text{H}_3)^+$, $(\text{C}_3)^+$,
 $(\text{C}_3\text{H})^+$ ions are observed, together with other ion peaks
 associated with hydrocarbon envelopes $(\text{C}_n\text{H}_m)^+$. Peaks at
 mass-to-charge ratios (m/z) 39 ($^{39}\text{K}^+$) and 41 ($^{41}\text{K}^+$)
 indicate the presence of K^+ . The peak at m/z 18 is assigned to NH_4^+ .
 Peaks at m/z 213 and 215 are assigned to potassium sulfate
 ions $^{213}(\text{K}_3\text{SO}_4)^+$ and $^{215}(\text{K}_3\text{SO}_4)^+$, respectively. The
 peak at m/z 97 is assigned to HSO_4^- (Figure 1b). The
 presence of sulfate on carbonaceous particles can result
 from direct emission by combustion sources, coagulation,
 cloud processing, and/or condensation and oxidation of
 sulfur dioxide on particles. Sulfate was usually observed
 in the carbonaceous particles detected during INDOEX
 (average sulfate associations for particles with aerodynamic
 diameters between 0.3 and 1.0 μm were determined to be
 75% for carbon-containing particles with K^+) [Guazzotti *et al.*,
 2001]. In the negative ion mass spectra of these
 particles, carbon ion clusters, such as C^- , $(\text{C}_2)^-$, $(\text{C}_3)^-$,
 and $(\text{C}_4)^-$, were periodically observed.

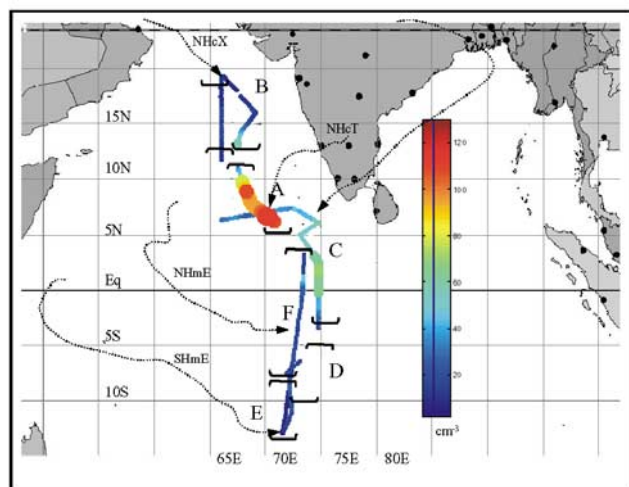


Figure 2. Spatial distribution of carbon-containing particles with potassium (aerodynamic diameter between 0.3 and 1.0 μm) along the cruise track of leg 2 of the NOAA R/V Ronald H. Brown. Regions A–F along the cruise track, impacted by different air mass source regions, are indicated together with typical 7-day back trajectories (ending at 950 hPa) indicative of the flow regimes described in the text.

[16] Particles are classified as carbon-containing with K^+ by carrying out exclusive searches in a Matlab[®] based database where threshold values (ion area, relative ion area, mass-to-charge ratios, etc.) for specific ions are specified. In this study, a relative area of greater than 10% for the peak at m/z 39 ($^{39}\text{K}^+$) is used for identification. The presence of a combination of at least two peaks at mass-to-charge ratios 12 (C^+), 36 (C_3^+), 48 (C_4^+), 60 (C_5^+), and 72 (C_6^+) with areas higher than 40 (arbitrary units) is required for these particles to be classified as carbon-containing with K^+ . Particles cannot be classified into more than one class (such as sea salt, dust, carbon-containing with no K^+ , etc.), therefore making the chemical classes exclusive. Once the particles are classified, their temporal evolution is evaluated and compared with results obtained with other techniques. In this classification scheme, no requirements are imposed in terms of ions that indicate the presence of sulfate and/or chloride, although one or both ions were observed in almost all of the mass spectra of the carbon-containing particles with K^+ . It has been previously shown that the presence of chloride and/or sulfate in combustion related particles depends on the temperature of formation of the particles as well as their aging process [e.g., Gaudichet et al., 1995; Ruellan et al., 1999; Liu et al., 2000]. For example, in the case of particles produced from biomass burning, Gaudichet et al. [1995] have indicated that near the emission sources more chlorine occurs in the observed soot particles than those collected farther downwind from the sources, indicating the evolution from KCl to K_2SO_4 .

[17] Figure 2 shows the spatial distribution of carbon-containing particles with K^+ along the cruise track for leg 2 of the INDOEX cruise. The cruise track was divided into 6 regions based on the geographical origin of the sampled air masses. These regions follow the classification of Ball et al. [2003] and are based on back trajectory analysis [Quinn et al., 2002]. The back trajectories were calculated using the

Hybrid Single-Particle Lagrangian Integrated Trajectory 420
 model (HY-SPLIT 4) [Draxler, 1991; Draxler and Hess, 421
 1998]. The six regimes encountered during leg 2 of the 422
 cruise, as indicated in Figure 2, are (A) Northern Hemi- 423
 sphere Continental Tropical (NHcT) (Indian Subcontinent 424
 air mass), (B) Northern Hemisphere Continental Extratrop- 425
 ical (NHcX) (Arabian Peninsula air mass), (C) Mixed 426
 Northern Hemisphere Continental (mixed NHc) (Arabian/ 427
 Indian Subcontinent air mass), (D) Northern Hemisphere 428
 Maritime Equatorial (NHmE) (Northern Indian Ocean air 429
 mass), (E) Southern Hemisphere Maritime Equatorial 430
 (SHmE) (Southern Indian Ocean air mass), and (F) North- 431
 ern Hemisphere Maritime Equatorial (Northern Indian 432
 Ocean air mass). Detailed explanations for the regimes 433
 described above are presented by Ball et al. [2003] and 434
 Mühle et al. [2002]. An overview of the regional meteor- 435
 ological circumstances during INDOEX-IFP is given by 436
 Verver et al. [2001]. 437

[18] The number concentration of carbon-containing par- 438
 ticles with K^+ was highest for the time period DOY 65.07– 439
 67.54, which corresponds to Region A (moving from 6.1°N 440
 71.3°E to 13.8°N 68.6°E). Region A was the most polluted 441
 based on the overall particle loading, aerosol optical depth, 442
 and trace gases mixing ratios [de Laat et al., 2001; Guazzotti 443
 et al., 2001; Ball et al., 2003; Mühle et al., 2002; Neusüß et 444
 al., 2002a; Quinn et al., 2002; Wisthaler et al., 2002]. In the 445
 northernmost region, Region B (DOY 68.08–69.85, mov- 446
 ing from 15.1°N 69.4°E to 19.0°N 67.1°E), a decrease in 447
 the number concentration of carbon-containing particles 448
 with K^+ was observed. During this period, the winds were 449
 mostly from the north. Back trajectories show general 450
 subsidence starting at 200–400 mbar above the Arabian 451
 Peninsula six days upwind subsiding to 950 mbar just one 452
 or two days before reaching the R/V Ronald H. Brown 453
 [Quinn et al., 2002]. In this region, an increase in the 454
 number concentration of dust particles [Guazzotti et al., 455
 2001] and in the mass concentration of nss Ca^{2+} and ash 456
 (noncombustible mineral dust) [Ball et al., 2003] was 457
 observed, indicating that the overall aerosol chemical 458
 composition had an influence from dust particles being trans- 459
 ported from the Middle East (K. R. Coffee et al., manuscript 460
 in preparation). In the southernmost locations, a decrease in 461
 the number concentration of carbon-containing particles 462
 with K^+ was observed (Region E, DOY 78.59–79.50). 463
 During that time period, the sampled air had no continental 464
 influence for 6 to 7 days, with the ITCZ located at 465
 approximately 12°S [Ball et al., 2003]. 466

3.2. Comparison of Single Particle Results to 467 Other Particle- and Gas-Phase Data sets 468

[19] In Figure 3, the observed temporal evolution of the 469
 number concentration of carbon-containing particles with K^+ 470
 is compared with the corresponding evolution of the mass 471
 concentration of submicrometer nss K^+ measured by two 472
 different research groups (PMEL and UMD) and the gas- 473
 phase acetonitrile mixing ratio. The same general trends are 474
 observed for both the particle- and gas-phase. The highest 475
 number concentration of carbon-containing particles with 476
 K^+ , mass concentration of submicrometer nss K^+ , and 477
 acetonitrile mixing ratio occurred during the time period 478
 DOY 65.07–67.54, Region A (average values 62 (± 16) 479
 cm^{-3} , 0.35 (± 0.14) $\mu\text{g m}^{-3}$, and 276 (± 9) pptv respectively). 480

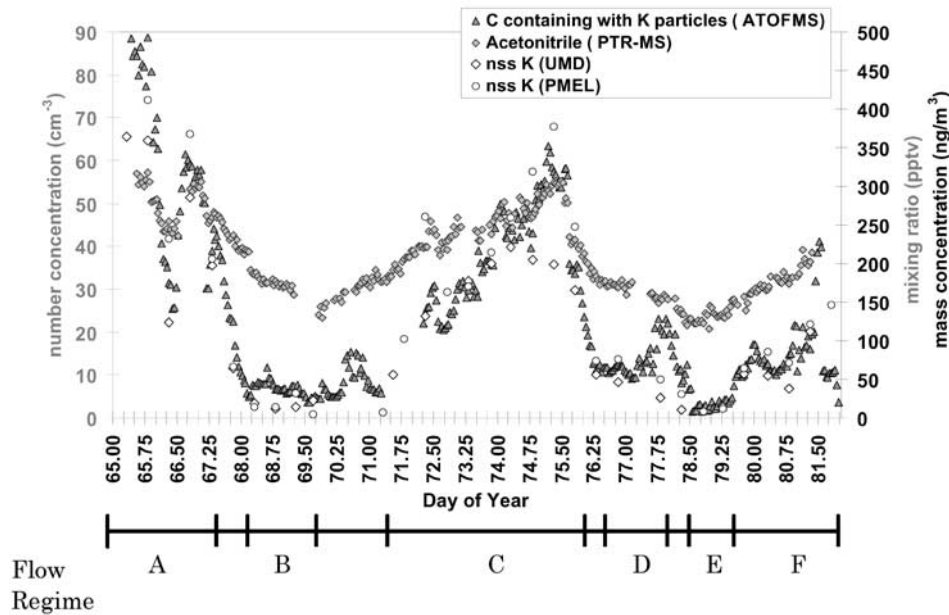


Figure 3. Temporal evolutions of submicrometer nss potassium mass concentration (PMEL and UMD), number concentration of carbon-containing particles with potassium, and acetonitrile mixing ratio observed during leg 2 of the INDOEX cruise.

481 The average values for the different regions are summarized
 482 in Table 1. In the northernmost locations (Region B, DOY
 483 68.08–69.85), a decrease is evident in all values (average
 484 values $7 (\pm 2) \text{ cm}^{-3}$, $0.017 (\pm 0.012) \mu\text{g}/\text{m}^3$, and $178 (\pm 18)$
 485 pptv) (see Table 1). As indicated, during this time the winds
 486 were mostly from the North, with air masses having an
 487 influence from the Arabian Peninsula. In the southernmost
 488 locations, when the sampled air mass had no continental
 489 influence for at least 6 to 7 days, decreases in the number
 490 concentrations of all species were observed. Average con-
 491 centrations decreased to their minimum observed values for
 492 the time period DOY 78.59–79.50 (see Table 1). Average
 493 number concentrations for particles with optical diameters
 494 between 0.3 and $1.0 \mu\text{m}$, as determined by an Optical Particle
 495 Counter (OPC) (Particle Measuring Systems, Inc.) aboard
 496 the R/V Ronald H. Brown, are also presented in Table 1 for
 497 comparison purposes. As shown in the Table, the same
 498 general trends discussed above apply to the overall number
 499 concentration of submicrometer particles. When compared
 500 to the values determined with the OPC, carbon-containing
 501 particles with K^+ represented 63 and 58% of the submi-
 502 crometer particles in Regions A and B, respectively. Aerosol
 503 number size distributions measured during the research
 504 cruise using a differential mobility particle sizer (DMPS)
 505 and an aerodynamic particle sizer (APS) are presented in
 506 Bates *et al.* [2002].

507 [20] Results from comparisons between submicrometer
 508 nss K^+ mass concentration measured by two different
 509 research groups (PMEL and UMD) show a high correlation
 510 factor between results ($r^2 = 0.91$), indicating that no partic-
 511 ular contamination or interference was experienced. The
 512 mass concentration values reported by UMD are consis-
 513 tently lower than those from PMEL due to the different size-
 514 cuts used for the corresponding evaluations ($0.74 \mu\text{m}$ and
 515 $1.0 \mu\text{m}$ respectively, see section 2.1). Mass concentration

values of submicrometer nss K^+ are highly correlated with
 the number concentration of carbon-containing particles
 with K^+ detected with ATOFMS ($r^2 = 0.92$). The high
 correlation indicates that most of the submicrometer nss
 K^+ was associated with carbonaceous material. A high
 correlation factor ($r^2 = 0.84$) is found between the number
 concentrations of carbon-containing particles with K^+ and
 gas-phase acetonitrile mixing ratios. Such good agreement
 is unexpected since deposition effects that govern the
 particle-phase would usually prevent the observation of a
 high correlation between gas- and particle-phase measure-
 ments of associated or related species. In particular, removal
 of particles from the lower troposphere due to precipitation
 has to be taken into consideration when comparing these
 results. Most of the data presented here were collected
 during time periods when no precipitation events occurred
 at the sampling site. Rain was encountered only near the
 ITCZ, where overall concentrations were low, and only a
 limited number of rain events were experienced during the
 air mass transport from the source. Lack of rain is typically
 experienced during the winter monsoon season [e.g., Rasch
et al., 2001]. The high correlation obtained for the number
 concentrations of submicrometer carbon-containing parti-
 cles with K^+ and the mixing ratios of acetonitrile most
 likely indicates that both arise from the same, related, or
 proximate sources. The correlation between the number
 concentration of carbon-containing particles with K^+ and
 the measured submicrometer absorption coefficient is eval-
 uated as well. The strong correlation ($r^2 = 0.92$) indicates
 that submicrometer carbon-containing particles with K^+ are
 most likely the major contributors to the observed absorp-
 tion. Neusiß *et al.* [2002a] arrived at similar conclusions
 from absorption and BC mass concentration measurements.
 Satheesh *et al.* [1999] suggested that BC from combustion
 sources is responsible for the strong absorption observed in

Table 1. Average Values Obtained for Different Air Masses and Flow Regimes^a

Region	Day of Year	Flow Regime ^b	Air Mass Type ^c	Absorption Coefficient, $M\ m^{-1}$	Nss K^+ , ^d $\mu g\ m^{-3}$	Acetonitrile, pptv	CewK, ^e cm^{-3}	Nss K^+/BC	Nss SO_4^{2-}/BC	BC/OC	Number Concentration, ^f cm^{-3}
t1.1											
t1.2	65.07–67.54	NHcT	Indian Subcontinent	11.4 (4.3)	0.35 (0.14)	276 (9)	62 (16)	0.4 (0.2)	7 (3)	1.5 (0.6)	99 (25)
t1.3	68.08–69.85	NHcX	Arabian Peninsula	0.97 (0.18)	0.017 (0.012)	178 (18)	7 (2)	0.18 ^g	11.8 ^g	0.22 ^g	12 (3)
t1.4	71.57–76.04	Mixed NHc	Arabian/Indian Subcontinent	6.4 (2.4)	0.24 (0.09)	248 (31)	39 (12)	0.5 (0.2)	9 (4)	1.2 (0.5)	55 (16)
t1.5	76.59–78.04	NHmE	Northern Indian Ocean	2.0 (0.4)	0.063 (0.018)	165 (9)	14 (4)	0.62 (0.04)	11 (4)	1.59 (0.02)	23 (6)
t1.6	78.59–79.50	SHmE	Southern Indian Ocean	0.50 (0.18)	0.0096 (0.0026)	132 (9)	3 (1)	N/A	N/A	N/A	12 (5)
t1.7	79.54–82.04	NHmE	Northern Indian Ocean	3.5 (2.1) ^h	0.098 (0.035)	176 (18) ⁱ	15 (7)	0.6 (0.2)	13 (4)	1.6 (0.4)	24 (11)
t1.8											

^aValues in parenthesis correspond to one standard deviation.

^bFlow regime classification as presented by *Ball et al.* [2003]: NHcT = Northern Hemisphere Continental Tropical; NHcX = Northern Hemisphere Continental Extra-Tropical; NHmE = Northern Hemisphere Maritime Equatorial.

^cAir Mass Type classification as presented by *Quinn et al.* [2002].

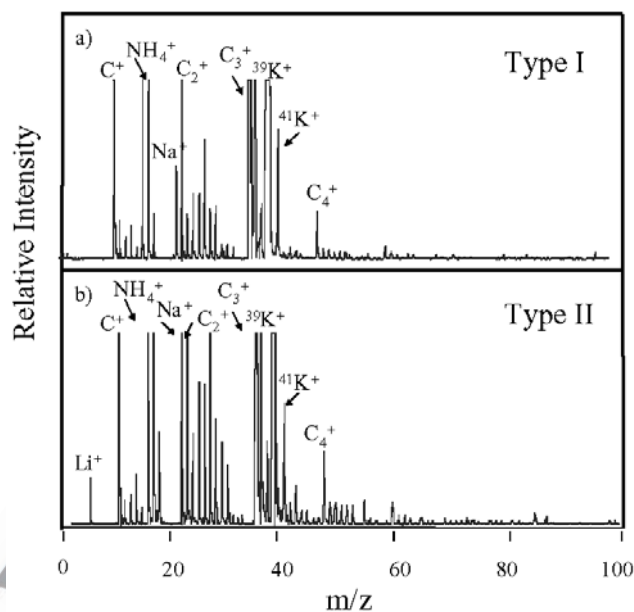
^dData from NOAA, Pacific Environmental Laboratory (PMEL).

^eCewK = carbon-containing particles with potassium.

^fAs determined with an Optical Particle Counter (OPC).

^gOnly one data point available for BC.

^hOnly up to DOY 81.98.

ⁱOnly up to DOY 81.35.

Figure 4. Representative positive ion mass spectra for carbon-containing particles of (a) Type I, and (b) Type II. Peak identifications correspond to the most probable assignments for each particular m/z ratio.

this area. Absorption due to aerosols in different regions sampled during INDOEX is discussed in detail in previous publications [e.g., *Clarke et al.* 2002; *Neusüß et al.* 2002a; *Quinn et al.* 2002].

3.3. Further Classification of Carbon-Containing Particles With Potassium

3.3.1. Carbon-Containing Particles With K^+ and Lithium

[21] ATOFMS single particle analysis allows for the identification of specific chemical species and combinations of species present in detected particles. In the case of carbon-containing particles with potassium, the presence of certain species can be used as an indication of the original source of the detected particles. From the characteristic mass spectra obtained for carbon-containing particles with K^+ , two major subclasses are identified, and their contributions to the aerosol chemical composition are evaluated. The main characteristics of the two subclasses are shown in Figure 4. For comparison purposes, only positive ion mass spectra of the different particle types up to m/z 100 are presented in Figure 4 since the presence of specific ion clusters in the positive ion mass spectra are used for the sub-classification. In most cases, the mass spectra were very reproducible (i.e., the major ion peaks were almost identical), indicating that the detected particles had originated from the same sources, or very similar sources in different locations, and/or that these particles had undergone similar aging processes. The positive ion mass spectrum presented in Figure 4a was obtained for a carbon-containing particle with K^+ denoted as Type I. The presence of K^+ is identified by peaks at m/z 39 and 41 ($^{39}K^+$ and $^{41}K^+$). Also a peak at m/z 18, due to NH_4^+ , appears in the respective positive ion mass spectrum. High concentrations of ammonium have been indicated for aerosol produced from biomass/biofuel

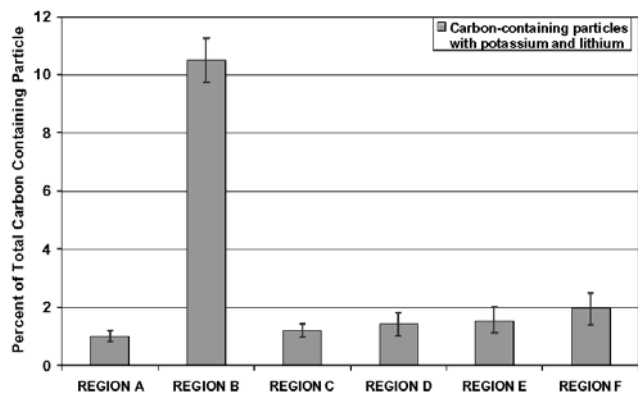


Figure 5. Contribution from carbon-containing particles with potassium and lithium (Type II) to the total number of carbon-containing particles in different regions sampled during INDOEX.

burning [e.g., Andreae and Crutzen, 1997]. Peaks at m/z 12, 24, 36, and 48, assigned to C^+ , $(C_2)^+$, $(C_3)^+$, and $(C_4)^+$, respectively, occur as well. In Figure 4b, a typical positive ion mass spectrum for a carbon-containing particle with K^+ of Type II is presented. The main difference with respect to particles of Type I is the presence of lithium (Li^+) at m/z 7 (and a peak due to sodium, Na^+ at m/z 23, with much higher relative intensity).

[22] The presence of lithium in carbonaceous particles could be an indicator of coal combustion. In combustion characterization experiments, lithium was almost never found in the single particle mass spectra of particles produced from biomass/biofuel burning (<0.3%) but it was commonly found in particles produced by coal combustion processes (D. T. Suess et al., manuscript in preparation). The characterization studies described by Suess et al. included several biomass/biofuel and coal sources relevant to the INDOEX study, which were analyzed by ATOFMS single particle analysis as well as by impactor bulk chemical analysis, therefore providing consistent data sets for comparison with the results obtained during the field campaign. Some of the biomass/biofuel sources investigated (of Bangladesh origin) included synthetic logs, dried coconut tree leaves, dried rice straw, and dried cow dung. Coal products studied included chunk coal from Bangladesh, China, India, and USA. It is important to mention that the studied chunk coals were ignited in a brick kiln, therefore producing combustion characteristics close to those commonly encountered in small-scale industrial processes and/or domestic use in India. As indicated by Reddy and Venkataraman [2001a], domestic coal combustion processes result in higher particle emissions than industrial ones, due to the lower temperatures used during combustion. Lithium can also be found in dust particles; however, the chemical characteristics of the dust particles are quite different from those arising from fossil fuel combustion sources (see, e.g., Guazzotti et al., 2001; K. R. Coffee et al., manuscript in preparation).

[23] Figure 5 shows the relative contribution of carbon-containing particles with K^+ and Li^+ (Type II) to the total carbon-containing particles. An increase in the contribution of Type II particles was observed for the period DOY

68.08–69.85 (Region B) along with a decrease in the contribution from particles of Type I. As mentioned, during this time period, the sampled air mass had an influence from the Arabian Peninsula. During this time, not only did the overall number concentration of carbon-containing particles with K^+ decrease, but a change in the chemical composition of observed particles occurred as well. Also, low values for the mass concentrations of submicrometer nss K^+ and gas-phase mixing ratios of acetonitrile are observed in this region.

3.3.2. Carbon-Containing Particles Without Potassium

[24] Not all submicrometer carbonaceous particles detected with the ATOFMS contain detectable amounts of potassium [Guazzotti et al., 2001]. The detection limit for potassium in a single particle by ATOFMS is approximately 3×10^{-18} g, this value being one of the lowest determined for several elements [Silva and Prather, 1997; Gross et al., 2000]. The relative contribution of carbon-containing particles with no detectable potassium to the total number of carbon-containing particles as observed in different regions is shown in Figure 6. Average contributions are in the range between 19 (± 6)% and 48 (± 18)%. These carbonaceous particles probably derived from the combustion of fossil fuels that contain little or no potassium, such as diesel. In Region B (Arabian influence), the contribution from carbonaceous particles with no detectable potassium (to the total number of carbon-containing particles) is higher than for the other regions. As mentioned above, this could be indicative of a change in the contribution from fossil fuel combustion emissions.

3.4. Single Particle Source Apportionment Estimates for the Contributions From Fossil Fuel Combustion and Biomass/Biofuel Burning to the Total Carbonaceous Aerosol

[25] Taking into consideration the results presented here, an attempt is made to estimate the relative contributions to the carbonaceous aerosol from particles emitted from biomass/biofuel burning with respect to those emitted from fossil fuel combustion. In order to estimate the contribution from particles emitted from biomass/biofuel burning, the

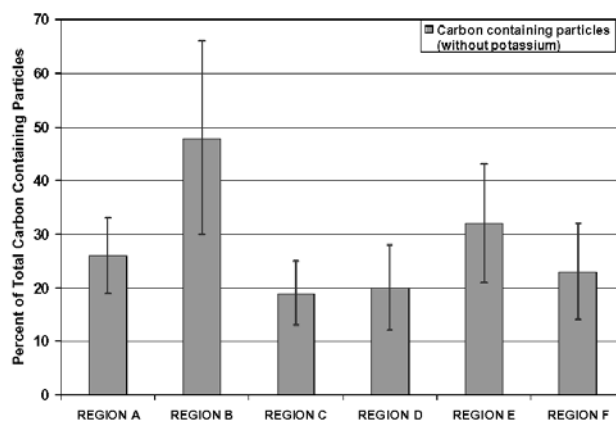


Figure 6. Contribution from carbon-containing particles (with no detectable amount of potassium) to the total number of carbon-containing particles in different regions sampled during INDOEX.

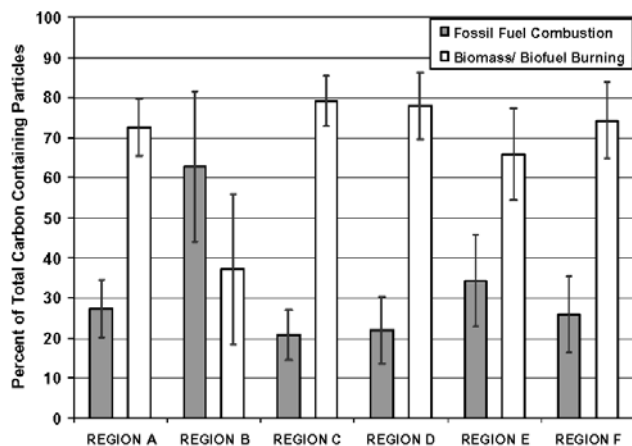


Figure 7. Single particle estimates of relative contributions from biomass/biofuel burning and fossil fuel combustion to the carbonaceous aerosol chemical composition in different regions. The contributions are evaluated as percentage of total carbon-containing particles with aerodynamic diameters between 0.3 and 1.0 μm .

667 proportion of carbon-containing particles with potassium
 668 and lithium (coal) is subtracted from the corresponding
 669 contribution from total carbon-containing particles with
 670 potassium. The relative contribution from particles emitted
 671 from fossil fuel sources is defined as the sum of the average
 672 contributions from carbon-containing particles with no
 673 detectable potassium (vehicular emissions and/or coal)
 674 and those from carbon-containing particles with potassium
 675 and lithium (coal). In these calculations, it is assumed that (1) all
 676 detected carbon-containing particles with potassium and
 677 lithium originate from coal combustion; (2) all carbon-
 678 containing particles with no detectable amount of potassium
 679 originate from vehicular emissions or other fossil fuel
 680 combustion sources that do not produce detectable amounts
 681 of potassium (e.g., particles emitted from coal combustion
 682 sources that do not contain potassium); and (3) all carbon-
 683 containing particles with potassium that do not contain
 684 lithium originate from biomass/biofuel burning sources.

685 [26] The estimates of relative contributions from particles
 686 emitted from biomass/biofuel burning and fossil fuel com-
 687 bustion are presented in Figure 7. A substantial change is
 688 observed in Region B (Arabian Influence) where the rela-
 689 tive contribution of particles emitted from fossil fuel com-
 690 bustion is the highest observed during leg 2, with an
 691 average value of 63 (± 19)%. This is in agreement with
 692 previously discussed results (section 3.2), where the domi-
 693 nance of fossil fuel has been indicated for that region. For
 694 the other regions (A, C–F), the contribution of particles
 695 emitted from fossil fuel combustion sources varied between
 696 20 and 34%, with an average value of 26 (± 9)%. For these
 697 regions, the estimated average contribution to the total
 698 carbonaceous particles from particles emitted from biomass
 699 sources varied between 73 to 79%, with an evaluated
 700 average of 74 (± 9)%.

701 [27] Reddy and Venkataraman [2001b] have indicated
 702 that for the INDOEX period (1998–1999), biomass/biofuel
 703 combustion was the major source of carbonaceous aerosols,
 704 based on an aerosol emission inventory for India for 1996–

1997. They have estimated that biomass/biofuel burning 705
 accounts for 71% of the black carbon emissions and 76% of 706
 the organic matter emissions. These estimates for biomass/ 707
 biofuel contributions are higher than those previously 708
 reported for 1990 [Reddy and Venkataraman, 2000]. The 709
 analysis presented by Dickerson *et al.* [2002] indicates that 710
 58–88% of the BC arises from biomass/biofuel burning. 711
 Our estimates, which correspond to the contributions in 712
 number of carbonaceous particles as determined during the 713
 field experiment in 1999, are in good agreement with the 714
 ones reported by Reddy and Venkataraman [2001b] and 715
 Dickerson *et al.* [2002]. From results obtained during three 716
 INDOEX research flights, Novakov *et al.* [2000] have 717
 estimated the contribution (in mass) of fossil fuel combus- 718
 tion to the carbonaceous aerosol to be approximately 80% 719
 using measured BC/TC ratios ($\text{TC} = \text{OC} + \text{BC}$) for their 720
 estimations. In our case, the contributions from different 721
 particle classes (with different chemical characteristics) to 722
 the carbonaceous aerosol chemical composition are consid- 723
 ered in the evaluation. The difference in results could be due 724
 to changes in the sampled air masses as well as in the actual 725
 sampling platform locations and times [Clarke *et al.*, 2002]. 726
 As mentioned, the results presented by Novakov *et al.* 727
 [2000] were derived from measurements on the C-130 728
 aircraft, whereas the results presented here were obtained 729
 on board the R/V Ronald H. Brown. Variability in air 730
 masses transport (e.g., long-range transport at high alti- 731
 tudes) and aerosol vertical structure could explain the 732
 different estimates. During the INDOEX sampling period, 733
 multiple particle layers of variable height and extension 734
 have been determined by a six-wavelength lidar [Müller *et al.*, 735
 2001a], showing vertical variability in aerosol properties 736
 [Müller *et al.*, 2001a, 2001b]. Measurements by a micro- 737
 pulse lidar system have shown that, during leg 2 of the 738
 INDOEX cruise, the marine boundary layer (MBL) was 739
 usually located below 1000 m with an aerosol layer aloft 740
 [Welton *et al.*, 2002]. Therefore the presence of a distinct 741
 aerosol layer above the MBL, with different chemical 742
 characteristics, could be expected. Also, it has been indi- 743
 cated that during INDOEX, the biomass/biofuel burning 744
 influence could have been stronger in the marine boundary 745
 layer than in the free troposphere [Reiner *et al.*, 2001], due 746
 to differences in the dominant aerosol sources near the 747
 surface and at higher altitudes [Rasch *et al.*, 2001]. Mete- 748
 orological conditions experienced during INDOEX-IFP can 749
 help explain the difference in outflow characteristics 750
 between the lower troposphere and the layers above the 751
 marine boundary layer [Verver *et al.*, 2001]. Also, temporal 752
 variations in the biomass/biofuel and fossil fuel contribu- 753
 tions to BC have been reported for a surface site in Goa, 754
 India [Alfaro *et al.*, 2002]. Based on measured nss K^+ and 755
 BC concentration values, and assuming a nss K^+ /BC ratio of 756
 0.52 for biomass/biofuel burning, Alfaro *et al.* [2002] 757
 estimated an increased biomass/biofuel influence in the 758
 surface site after 10 March 1999 (e.g., as much as 70% of 759
 the BC was estimated to arise from biomass/biofuel burning 760
 around 23 March versus only 30% for early March 1999). 761

[28] The calculated contributions of carbonaceous parti- 762
 cles from biomass/biofuel burning should be considered as 763
 upper estimates, in particular for Region B. There is a 764
 possibility that the contributions from carbon-containing 765
 particles with K^+ that do not contain Li^+ , arising from local 766

coal sources, are higher than those evaluated from source characterization studies (D. T. Suess, manuscript in preparation). Also, it could be possible that the ATOFMS technique was unable to detect the presence of Li^+ in some carbon-containing particles with K^+ that contained Li^+ in trace amounts below the detection threshold. The presence of specific markers in the mass spectra of individual particles, such as Li^+ , can be used to refine the estimates, but further characterization studies of single particles produced from combustion processes are necessary for proper assessment. The results presented here for the assignment of possible particle sources from characterization studies represent a first step in the ultimate goal of using single particle signatures for source apportionment. The high correlation found for the number concentration of submicrometer carbon-containing particles with K^+ and the mixing ratio of acetonitrile also indicates that the majority of the carbon-containing particles with K^+ most likely arise from biomass/biofuel burning. Results from other measurements (e.g., trace gases, nonmethane hydrocarbons, CO, CO isotopic ratios [Mühle *et al.*, 2002; Wisthaler *et al.*, 2002]) and source analysis (e.g., source analysis for CO [de Laat *et al.*, 2001]) further support the conclusions presented for leg 2 of the INDOEX cruise.

3.5. Ratios Between Chemical Species in Different Regions

[29] Ratios between different chemical species, for the regions described in the text, are evaluated and presented in this section. Their values are discussed as indications of probable sources (i.e., biomass/biofuel burning and fossil fuel combustion) and compared, when appropriate, with results presented in previous sections.

3.5.1. Nss K^+ /BC Ratio

[30] The average submicrometer nss K^+ /BC ratios are evaluated for the different regimes from results of submicrometer mass concentration of BC and nss K^+ , as described in sections 2.1 and 2.2 respectively. For the time period DOY 65.07–67.54 (Region A) the average value is determined to be 0.4, whereas for the time period DOY 68.08–69.85 (Region B), the nss K^+ /BC ratio has an average value of 0.18. Higher nss K^+ /BC ratios in the range between 0.5 and 0.62 are obtained for the remaining regions (Table 1). The relatively high nss K^+ /BC ratios indicate that the sampled air masses were probably impacted by biomass/biofuel burning. Reported values for K^+ /BC ratios obtained from biomass/biofuel burning are usually in the range between 0.2 and 1.1 depending on the type of fire, the sampled region, and the size of the particles considered for the evaluation [e.g., Andreae, 1983; Ferek *et al.*, 1998; Maenhaut *et al.*, 1996; Reid *et al.*, 1998; Yamasoe *et al.*, 2000; Andreae and Merlet, 2001]. In urban areas, the encountered nss K^+ /BC ratios are low (0.025 to 0.09 in the US) [Stevens *et al.*, 1980; Andreae, 1983]. For urban, industrial, and rural areas in Pakistan, Smith *et al.* [1996] have reported K^+ /BC ratios of 0.23 for particles with diameters smaller than 10 μm . It has been previously reported that fossil fuel combustion generates little potassium [Andreae, 1983], with K^+ /BC ratios for fuel oil combustion being as low as 10^{-5} [Winchester and Nifong, 1971]. Diesel and gasoline engines also produce only small amounts of K^+ [Andreae, 1983]. The low submicrometer

nss K^+ /BC ratio (0.18) found in the Arabian air mass (Region B) could be indicative of an increase in the contribution from fossil fuel combustion. A decrease in the relative NH_4^+ concentration has been reported as indicative of a decrease in the relative contribution of particles from biomass/biofuel burning in this region [Ball *et al.*, 2003]. The contribution to BC from biomass/biofuel burning can be estimated using measured nss K^+ and BC values and a typical nss K^+ /BC ratio value of 0.52 (± 11) for biomass/biofuel burning (at the source) [Cachier *et al.*, 1991; Ferek *et al.*, 1998], in a similar manner to that carried out by Alfaro *et al.* [2002] (i.e., contribution to BC from biomass/biofuel = $100 \cdot ((\text{nss } \text{K}^+ / 0.52) / \text{BC})$). Results from this evaluation yield biomass/biofuel burning contributions to BC of 77% for Region A, 35% for Region B, and 96% for Region C. These values, as well as the corresponding nss K^+ /BC ratios, are consistent with the estimates for the contributions from biomass/biofuel burning presented in section 3.4.

3.5.2. Acetonitrile/CO Ratio

[31] As mentioned, acetonitrile is a unique, long-lived tracer for biomass/biofuel burning [e.g., Lobert *et al.*, 1990; Holzinger *et al.*, 1999; Bange and Williams, 2000]. Industrial emissions and fossil fuel combustion are only minor sources of acetonitrile [e.g., Arijis and Brasseur, 1986; Holzinger *et al.*, 2001]. CO is a general marker for incomplete combustion including fossil fuel combustion and biomass/biofuel burning. The evaluation of the acetonitrile/CO enhancement ratio ($\Delta\text{CH}_3\text{CN}/\Delta\text{CO}$) for different air masses encountered during leg 2 of the INDOEX cruise is presented in detail by Wisthaler *et al.* [2002]. Since both trace gases are relatively long-lived, the observed $\Delta\text{CH}_3\text{CN}/\Delta\text{CO}$ enhancement ratio is expected to reflect the source characteristic emission ratio. In air masses from Western India (part of Regions A and C), a $\Delta\text{CH}_3\text{CN}/\Delta\text{CO}$ enhancement ratio of 0.0024 was observed. Laboratory studies of controlled biomass fires covering a large variety of different types of biofuel [Lobert *et al.*, 1991] yielded a mean primary molar emission ratio $\Delta\text{CH}_3\text{CN}/\Delta\text{CO}$ of 0.0025. The strong correlation between CO and acetonitrile ($R^2 = 0.87$) and the similarity of enhancement ratio to the primary emission ratio observed by Lobert *et al.* [1991] indicate that biomass/biofuel burning most likely dominated CO emissions in these regions, which is in agreement with results presented in section 3.4. In the Arabian air mass (Region B), acetonitrile mixing ratios decreased to southern hemispheric background values (see Figure 3) and were not correlated with increasing CO levels [Stehr *et al.*, 2002]. These findings suggest that fossil fuel combustion was the primary source of CO in the Arabian air parcels. From results of single particle apportionment, high contributions from particles emitted from fossil fuel combustion were observed in this region as well (section 3.4).

3.5.3. BC/OC Ratio

[32] As shown in Table 1, high BC/OC ratios for submicrometer particles, in the range between 1.55 and 1.61, were found in all regions with exception of Region B (0.22). These ratios are higher than normally expected solely from biomass/biofuel burning or fossil fuel emissions. For example, from the $\text{PM}_{2.5}$ emission inventory for India [1990] provided by Reddy and Venkataraman [2000], a BC/OC ratio of 0.18–0.27 for fossil fuels, and 0.08–0.22

890 for biomass/biofuel burning can be derived. From the data
 891 compiled by *Andreae and Merlet* [2001] BC/OC ratios of
 892 0.07–0.3 can be determined for various types biomass/
 893 biofuel burning. It has been suggested that the high BC/OC
 894 ratio observed during INDOEX could mostly be due to
 895 emissions of black carbon from fossil fuel combustion
 896 processes [*Novakov et al.*, 2000]. High BC emissions are
 897 expected for emissions from diesel engines [*Kleeman et*
 898 *al.*, 2000] and certain coal combustion processes (D. T.
 899 Suess et al., manuscript in preparation). Some investigators
 900 have indicated that known emission factors for fossil fuel
 901 cannot account for the high BC concentration values
 902 encountered in the region [*Dickerson et al.*, 2002]. In
 903 India, biomass/biofuel combustion is considered a major
 904 source for carbonaceous aerosol, accounting for 71% of the
 905 total BC emissions [*Reddy and Venkataraman*, 2001b]. It is
 906 reasonable to expect a substantial amount of BC to
 907 originate from biomass/biofuel burning since a positive
 908 correlation between BC and CO has been observed in
 909 South Asia [*Dickerson et al.*, 2002], and source analysis of
 910 CO pollution has found biofuel and agricultural waste
 911 burning to be major sources of CO in the region [*de Laat*
 912 *et al.*, 2001]. As previously mentioned, due to the techni-
 913 que employed, the BC concentration values presented here
 914 are considered upper limits (see section 2.2) [*Chow et al.*,
 915 2001].

3.5.4. Nss SO_4^{2-} /BC Ratio

917 [33] The ratios between submicrometer nss sulfate and
 918 BC (nss SO_4^{2-} /BC) are evaluated for the different regimes,
 919 and the results are summarized in Table 1. The large average
 920 values obtained for this ratio for all regions are indicative of
 921 the importance of direct emissions and aged particles.
 922 Generally, nss SO_4^{2-} is used as tracer for fossil fuel com-
 923 bustion, since only small emissions of sulfate are normally
 924 reported for biomass/biofuel burning [e.g., *Crutzen and*
 925 *Andreae*, 1990; *Thornton et al.*, 1999]. Based on the sulfate
 926 mass content, a substantial fraction of the total (not only
 927 carbonaceous) aerosol mass sampled during INDOEX has
 928 been reported to be due to fossil fuel combustion [*Reiner et*
 929 *al.*, 2001; *Lelieveld et al.*, 2001]. However, differences in
 930 the estimates of sulfur emissions due to biofuel sources in
 931 India are substantial, in particular for cattle dung-cake
 932 which produces SO_2 emissions higher than other biofuel
 933 sources [*Arndt et al.*, 1997; *Smith et al.*, 2000; *Reddy and*
 934 *Venkataraman*, 2001b]. Also, it has been indicated that
 935 biofuel burning can be the dominant contributor to regional
 936 SO_2 emissions in a number of developing countries [*Streets*
 937 *and Waldhoff*, 1999]. Sulfur emissions from shipping ves-
 938 sels have been indicated as possible important contributors
 939 to SO_2 emissions as well [*Streets et al.*, 2000; *Mayol-*
 940 *Bracero et al.*, 2002]. This could also account for the
 941 higher nss SO_4^{2-} /BC ratios determined from the samples
 942 collected aboard the R/V Ronald H. Brown when compared
 943 with those from the NCAR C-130 aircraft (e.g., ratios
 944 between 1.3 and 2.8 have been reported for different
 945 flights) [*Novakov et al.*, 2002; *Clarke et al.*, 2002; *Mayol-*
 946 *Bracero et al.*, 2002].

4. Conclusions

948 [34] Results obtained by traditional standardized aerosol
 949 particle chemical analysis, real-time single-particle analysis,

and fast-response gas-phase PTR-MS reflect the impact of
 different meteorological regimes and air masses encoun-
 tered during leg 2 of the R/V Ronald H. Brown INDOEX
 cruise. Low overall concentrations are found in the south-
 ernmost regions sampled where the air masses did not have
 any recent land influence. High values for concentration of
 submicrometer nss K^+ , carbon-containing particles with K^+ ,
 acetonitrile mixing ratio, and submicrometer nss K^+ /EC
 ratios are observed in air masses advected from India.
 Results from an extended set of measurements imply a high
 contribution to carbonaceous aerosols from biomass/biofuel
 burning (accounting for approximately 75% of the carbon-
 containing particles), even in areas far from sources, show-
 ing the possibility of long-range transport (up to 7 days, as
 indicated by back trajectory analysis).

[35] In air parcels from the Arabian Peninsula, the
 overall number concentration of carbon-containing parti-
 cles with K^+ , the submicrometer nss K^+ mass concen-
 tration, and the acetonitrile mixing ratio decreased
 resulting in a smaller nss K^+ /EC and acetonitrile/CO ratio.
 These findings indicate a reduced biomass/biofuel burning
 impact and a higher contribution from fossil fuel combus-
 tion. A higher relative contribution from carbon-containing
 particles with K^+ and Li^+ indicate a higher relative con-
 tribution of carbonaceous particles from coal combustion
 derived particles, since carbon-containing particles with
 potassium and lithium have been observed in related
 source characterization studies. Also, carbon-containing
 particles with no detectable amount of potassium were
 enhanced in this region, indicating a stronger impact from
 fossil fuel combustion. Future studies involving further
 chemical characterization from different sources will be
 essential for minimizing some of the uncertainties, allow-
 ing for proper assessments of Asia's pollution impact on
 regional and global scales.

[36] **Acknowledgments.** This work was supported in part by: the
 National Science Foundation via the Center for Clouds Chemistry and
 Climate (C^4) at the Scripps Institution of Oceanography under Grants ATM-
 9612887 and ATM-9405024; the Aerosol Project of the NOAA Climate and
 Global Change Program; the Global Aerosol Climatology Project of the
 NASA Earth System Science Program; and the Bundesministerium für
 Bildung, Wissenschaft, Forschung und Technik (BMBF) under contract
 LA-9830/0. We thank the captain and crew of the NOAA R/V Ronald H.
 Brown for their help and support.

References

- Alfaro, S. C., A. Gaudichet, J. L. Rajot, L. Gomes, M. Maille, and
 H. Cachier, Variability of aerosol size-resolved composition at an Indian
 coastal site during INDOEX intensive field phase, *J. Geophys. Res.*,
 108(D8), 4235, doi:10.1029/2002JD002645, 2002.
 Allen, J. O., D. P. Fergenson, E. E. Gard, L. S. Hughes, B. D. Morrical,
 M. J. Kleeman, D. S. Gross, M. E. Galli, K. A. Prather, and G. R. Cass,
 Particle detection efficiencies of aerosol time of flight mass spectrometers
 under ambient sampling conditions, *Environ. Sci. Technol.*, 34(1), 211–
 217, 2000.
 Anderson, T. L., D. S. Covert, J. D. Wheeler, J. M. Harris, K. D. Perry, B. E.
 Trost, D. J. Jaffe, and J. A. Ogren, Aerosol backscatter fraction and single
 scattering albedo: Measured values and uncertainties at a coastal station
 in the Pacific Northwest, *J. Geophys. Res.*, 104(D21), 26,793–26,807,
 1999.
 Andreae, M. O., Soot carbon and excess fine potassium: Long-range
 transport of combustion-derived aerosols, *Science*, 220, 1148–1151,
 1983.
 Andreae, M. O., Biomass burning: Its history, use, and distribution and its
 impact on environmental quality and global climate, in *Global Biomass*
Burning: Atmospheric, Climatic and Biospheric Implications, edited by
 J. S. Levine, pp. 3–21, MIT Press, Cambridge, Mass., 1991.

- 1016 Andreae, M. O., and P. J. Crutzen, Atmospheric aerosols: Biogeochemical
1017 sources and role in atmospheric chemistry, *Science*, 276(5315), 1052–
1018 1058, 1997.
- 1019 Andreae, M. O., and P. Merlet, Emissions of trace gases and aerosols from
1020 biomass burning, *Global Biogeochem. Cycles*, 15, 955–966, 2001.
- 1021 Andreae, M. O., E. Atlas, H. Cachier, W. R. Cofer III, G. W. Harris,
1022 G. Helas, R. Kopppmann, J.-P. Lacaux, and D. E. Ward, Trace gas and
1023 aerosol emissions from savanna fires, in *Biomass Burning and Global
1024 Change*, vol. 1, edited by J. S. Levine, pp. 278–295, MIT Press, Cam-
1025 bridge, Mass., 1996.
- 1026 Arijs, E., and G. Brasseur, Acetonitrile in the stratosphere and implication
1027 for positive ion composition, *J. Geophys. Res.*, 91, 4003–4016, 1986.
- 1028 Arndt, R. L., G. R. Carmichael, D. G. Streets, and N. Bhatti, Sulfur dioxide
1029 emissions and sectorial contributions to sulfur deposition in Asia, *Atmos.
1030 Environ.*, 31, 1553–1572, 1997.
- 1031 Ball, W. P., R. R. Dickerson, B. G. Doddridge, J. W. Stehr, T. L. Miller,
1032 D. L. Savoie, and T. P. Carsey, Bulk and size-segregated aerosol com-
1033 position observed during INDOEX 1999: Overview of meteorology and
1034 continental impacts, *J. Geophys. Res.*, 108(D10), 8001, doi:10.1029/
1035 2002JD002467, 2003.
- 1036 Bange, H. W., and J. Williams, New Directions: Acetonitrile in atmospheric
1037 and biogeochemical cycles, *Atmos. Environ.*, 34(28), 4959–4960, 2000.
- 1038 Bates, T. S., D. J. Coffman, D. S. Covert, and P. K. Quinn, Regional marine
1039 boundary layer aerosol size distributions in the Indian, Atlantic, and
1040 Pacific Oceans: A comparison of INDOEX measurements with ACE-1,
1041 ACE-2, and Aerosols99, *J. Geophys. Res.*, 107(D9), 8026, doi:10.1029/
1042 2001JD001174, 2002.
- 1043 Berner, A., C. Lurzer, F. Pohl, O. Preining, and P. Wagner, The size dis-
1044 tribution of the urban aerosol in Vienna, *Sci. Total Environ.*, 13, 245–
1045 261, 1979.
- 1046 Bond, T. C., T. L. Anderson, and D. Campbell, Calibration and intercom-
1047 parison of filter-based measurements of visible light absorption by aer-
1048 osols, *Aerosol Sci. Technol.*, 30(6), 82–600, 1999.
- 1049 Cachier, H., and J. Ducret, Influence of biomass burning on equatorial
1050 African rains, *Nature*, 352(6332), 228–230, 1991.
- 1051 Cachier, H., M. P. Bremond, and P. Buat-Menard, Carbonaceous aerosols
1052 from different tropical biomass burning sources, *Nature*, 340(6232),
1053 371–373, 1989.
- 1054 Cachier, H., J. Ducret, M. P. Bremond, A. Gaudichet, V. Yoboue, J. P.
1055 Lacaux, and J. Baudet, in *Global Biomass Burning: Atmospheric, Cli-
1056 matic, and Biospheric Implications*, edited by J. S. Levine, pp. 174–180,
1057 MIT Press, Cambridge, Mass., 1991.
- 1058 Cadle, S. H., and P. A. Mulawa, Atmospheric carbonaceous species mea-
1059 surement methods comparison study: General Motors results, *Aerosol
1060 Sci. Technol.*, 12, 128–141, 1990.
- 1061 Charlson, R. J., J. Langner, H. Rodhe, C. B. Leovy, and S. G. Warren,
1062 Perturbation of the northern hemisphere radiative balance by backscatter-
1063 ing from anthropogenic sulfate aerosols, *Tellus, Ser. A*, 43(4), 152–163,
1064 1991.
- 1065 Chow, J. C., J. G. Watson, D. Crow, D. H. Lowenthal, and T. Merrifield,
1066 Comparison of IMPROVE and NIOSH carbon measurements, *Aerosol
1067 Sci. Technol.*, 34, 23–34, 2001.
- 1068 Clarke, A., et al., INDOEX aerosol: A comparison and summary of micro-
1069 physical, chemical and optical properties observed from land, ship and
1070 aircraft, *J. Geophys. Res.*, 107(D19), 8033, doi:10.1029/2001JD000572,
1071 2002.
- 1072 Coakley, J. A., and R. D. Cess, Response of the NCAR community climate
1073 model to the radiative forcing by the naturally-occurring tropospheric
1074 aerosol, *J. Atmos. Sci.*, 42, 1677–1692, 1985.
- 1075 Cooke, W. F., and J. J. N. Wilson, A global black carbon aerosol model,
1076 *J. Geophys. Res.*, 101(D14), 19,395–19,409, 1996.
- 1077 Countes, R. J., Interlaboratory analyses of carbonaceous samples, *Aerosol
1078 Sci. Technol.*, 12, 114–121, 1990.
- 1079 Crutzen, P. J., and M. O. Andreae, Biomass burning in the tropics:
1080 Impact on atmospheric chemistry and biogeochemical cycles, *Science*,
1081 250(4988), 1669–1678, 1990.
- 1082 de Laat, A. T. J., J. Lelieveld, G. J. Roelofs, R. R. Dickerson, and J. M.
1083 Lobert, Source analysis of carbon monoxide during INDOEX 1999,
1084 *J. Geophys. Res.*, 106, 28,481–28,495, 2001.
- 1085 Desalmand, F., R. Serpelay, and J. Podzimek, Some specific features of
1086 the aerosol particle concentrations during the dry season and during a
1087 bushfire event in West Africa, *Atmos. Environ.*, 19, 1535–1543, 1985.
- 1088 Dickerson, R. R., M. O. Andreae, T. Campos, O. L. Mayol-Bracero,
1089 C. Neusuess, and D. G. Streets, Analysis of black carbon and carbon
1090 monoxide observed over the Indian Ocean: Implications for emissions
1091 and photochemistry, *J. Geophys. Res.*, 107(D9), 8017, doi:10.1029/
1092 2001JD000501, 2002.
- 1093 Draxler, R. R., The accuracy of trajectories during Anatex calculated using
1094 dynamic model analyses versus rawinsonde observations, *J. Appl. Me-
1095 teorol.*, 30(10), 1446–1467, 1991.
- Draxler, R. R., and G. D. Hess, An overview of the Hysplit 4 modeling
system for trajectories, dispersion and deposition, *Aust. Meteorol. Mag.*,
47, 295–308, 1998.
- Ferek, R. J., J. S. Reid, P. V. Hobbs, D. R. Blake, and C. Lioussé, Emission
factors of hydrocarbons, halocarbons, trace gases and particles from bio-
mass burning in Brazil, *J. Geophys. Res.*, 103(D24), 32,107–32,118,
1998.
- Gard, E., J. E. Mayer, B. D. Morrical, T. Dienes, D. P. Fergenson, and K. A.
Prather, Real-time analysis of individual atmospheric aerosol particles:
Design and performance of a portable ATOFMS, *Anal. Chem.*, 69(20),
4083–4091, 1997.
- Gaudichet, A., F. Echalar, B. Chatenet, J.P. Quisefit, G. Malingre, H. Cach-
ier, P. Buat-Menard, P. Artaxo, and W. Maenhaut, Trace elements in
tropical African Savanna biomass burning aerosols, *J. Atmos. Chem.*,
22(1–2), 19–39, 1995.
- Gross, D. S., M. E. Galli, P. J. Silva, and K. A. Prather, Relative sensitivity
factors for alkali metal and ammonium cations in single particle aerosol
time-of-flight mass spectra, *Anal. Chem.*, 72(2), 416–422, 2000.
- Guazzotti, S. R., K. R. Coffee, and K. A. Prather, Continuous measure-
ments of size resolved particle chemistry during INDOEX-IFP 99,
J. Geophys. Res., 106(22), 28,607–28,627, 2001.
- Hall, D. O., F. Rosilloccalle, and J. Woods, Biomass utilization in house-
holds and industry: Energy use and development, *Chemosphere*, 29(5),
1099–1119, 1994.
- Hall, D. O., G. W. Barnar, and P. A. Moss, *Biomass for Energy in the
Developing Countries*, Pergamon, New York, 1992.
- Hallett, J., J. G. Hudson, and C. F. Rogers, Characterization of combustion
aerosols for haze and cloud formation, *Aerosol Sci. Technol.*, 10, 70–83,
1989.
- Hansel, A., A. Jordan, R. Holzinger, P. Prazeller, W. Vogel, and W. Lind-
inger, Proton transfer reaction mass spectrometry: On-line trace gas
analysis at the ppbv level, *Int. J. Mass Spectrom. Ion Processes*, 149/
150, 609–619, 1995.
- Haywood, J., and O. Boucher, Estimates of the direct and indirect radiative
forcing due to tropospheric aerosols: A review, *Rev. Geophys.*, 38(4),
513–543, 2000.
- Haywood, J. M., and K. P. Shine, Multi-spectral calculations of the
direct radiative forcing of tropospheric sulphate and soot aerosols
using a column model, *Q. J. R. Meteorol. Soc.*, 123(543), 1907–
1930, 1997.
- Haywood, J. M., and K. P. Shine, The effect of anthropogenic sulfate and
soot aerosol on the clear sky planetary radiation budget, *Geophys. Res.
Lett.*, 22(5), 603–606, 1995.
- Haywood, J. M., D. L. Roberts, A. Slingo, J. M. Edwards, and K. P. Shine,
General circulation model calculations of the direct radiative forcing by
anthropogenic sulfate and fossil-fuel soot aerosol, *J. Clim.*, 10(7), 1562–
1577, 1997.
- Holzinger, R., A. Jordan, A. Hansel, and W. Lindinger, Automobile emis-
sions of acetonitrile: Assessment of its contribution to the global source,
J. Atmos. Chem., 38(2), 187–193, 2001.
- Holzinger, R., C. Warneke, A. Hansel, A. Jordan, W. Lindinger, D. H.
Scharffe, G. Schade, and P. J. Crutzen, Biomass burning as a source of
formaldehyde, acetaldehyde, methanol, acetone, acetonitrile, and hydro-
gen cyanide, *Geophys. Res. Lett.*, 26(8), 1161–1164, 1999.
- Howell, S., A. A. P. Pszeny, P. Quinn, and B. Huebert, A field intercom-
parison of three cascade impactors, *Aerosol Sci. Technol.*, 29(6), 475–
492, 1998.
- Hughes, L. S., et al., Size and composition distribution of atmospheric
particles in southern California, *Environ. Sci. Technol.*, 33(20), 3506–
3515, 1999.
- Intergovernmental Panel on Climate Change (IPCC), Climate change,
1995: The science of climate change, Cambridge Univ. Press, New York,
1996.
- Iversen, T., and L. Tarrason, On climatic effects of arctic aerosols, *Inst. Rep.
Ser., Report No. 94*, Dep. of Geophysics, Oslo, Norway, 1995.
- Iversen, T., A. Kirkevåg, and O. Seland, Hemispheric modeling of sulphate
and black carbon and their direct effects, in *Air Pollution Modeling and
its Applications, XII*, edited by C. Grynning, pp. 477–480, Plenum Press,
New York, 1998.
- Jacobson, M. Z., Strong radiative heating due to the mixing state of black
carbon in atmospheric aerosols, *Nature*, 409(6821), 695–697, 2001.
- Kleeman, M. J., J. J. Schauer, and G. R. Cass, Size and composition dis-
tribution of fine particulate matter emitted from motor vehicles, *Environ.
Sci. Technol.*, 34(7), 1132–1142, 2000.
- Kuhlbusch, T. A. J., M. O. Andreae, H. Cachier, J. G. Goldammer, J. P.
Lacaux, R. Shea, and P. J. Crutzen, Black carbon formation by Savanna
fires: Measurements and implications for the global carbon cycle,
J. Geophys. Res., 101(D19), 23,651–23,665, 1996.
- Lelieveld, J., et al., The Indian Ocean experiment: Widespread air pollution
from South and Southeast Asia, *Science*, 291, 1031–1036, 2001.

- 1176 Lindinger, W., A. Hansel, and A. Jordan, Proton-transfer-reaction mass
1177 spectrometry (PTR-MS): On-line monitoring of volatile organic com-
1178 pounds at pptv levels, *Chem. Soc. Rev.*, 27, 347–354, 1998.
- 1179 Liu, X. D., P. Van Espen, F. Adams, J. Cafmeyer, and W. Maenhaut,
1180 Biomass burning in southern Africa: Individual particle characterization
1181 of atmospheric aerosols and savanna fire samples, *J. Atmos. Chem.*, 36,
1182 135–155, 2000.
- 1183 Lobert, J. M., D. H. Scharffe, W. M. Hao, and P. J. Crutzen, Importance of
1184 biomass burning in the atmospheric budgets of nitrogen-containing gases,
1185 *Nature*, 346(6284), 552–554, 1990.
- 1186 Lobert, J. M., et al., Experimental evaluation of biomass burning emis-
1187 sions: Nitrogen and carbon containing compounds, in *Global Biomass*
1188 *Burning: Atmospheric, Climatic, and Biospheric Implications*, edited by
1189 J. S. Levine, pp. 289–303, MIT Press, Cambridge, Mass., 1991.
- 1190 Maenhaut, W., I. Salma, J. Cafmeyer, H. J. Annegam, and M. O. Andreae,
1191 Regional atmospheric aerosol composition and sources in the eastern
1192 Transvaal, South Africa, and impact of biomass burning, *J. Geophys.*
1193 *Res.*, 101(D19), 23,631–23,650, 1996.
- 1194 Mayol-Bracero, O. L., R. Gabriel, M. O. Andreae, T. W. Kirchstetter,
1195 T. Novakov, and D. G. Streets, Carbonaceous aerosols over the Indian
1196 Ocean during INDOEX: Chemical characterization, optical properties,
1197 and probable sources, *J. Geophys. Res.*, 107(D19), 8030, doi:10.1029/
1198 2000JD000039, 2002.
- 1199 Mitra, A. P., INDOEX (India): Introductory note, *Curr. Sci.*, 76(7), 886–
1200 889, 1999.
- 1201 Mühle, J., A. Zahn, C. A. M. Brenninkmeijer, V. Gros, and P. J. Crutzen,
1202 Air mass classification during INDOEX R/V Ronald Brown cruise
1203 using measurements of nonmethane hydrocarbons, CH₄, CO₂, CO,
1204 ¹⁴C, and δ¹⁸O (CO), *J. Geophys. Res.*, 107(D19), 8021, doi:10.1029/
1205 2001JD000730, 2002.
- 1206 Müller, D., K. Franke, F. Wagner, D. Althausen, A. Ansmann, and
1207 J. Heintzenberg, Vertical profiling of optical particle properties over
1208 the tropical Indian Ocean with six-wavelength lidar: 1. Seasonal cycle,
1209 *J. Geophys. Res.*, 106, 28,567–28,575, 2001a.
- 1210 Müller, D., K. Franke, F. Wagner, D. Althausen, A. Ansmann, and
1211 J. Heintzenberg, Vertical profiling of optical particle properties over the
1212 tropical Indian Ocean with six-wavelength lidar: 2. Case studies,
1213 *J. Geophys. Res.*, 106, 28,577–28,595, 2001b.
- 1214 Neusüß, C., T. Gnauk, A. Plewka, H. Herrmann, and P. K. Quinn, Carbo-
1215 naceous aerosol over the Indian Ocean: OC/EC fractions and selected
1216 specifications from size-segregated onboard samples, *J. Geophys. Res.*,
1217 107(D19), 8031, doi:10.1029/2001JD000327, 2002a.
- 1218 Neusüß, C., H. Wex, W. Birmili, A. Wiedensohler, C. Kozian, B. Busch,
1219 E. Brüggemann, and T. Gnauk, Characterization and parameterization of
1220 atmospheric particle number-, mass-, and chemical-size distributions in
1221 central Europe during LACE 98 and MINT, *J. Geophys. Res.*,
1222 107(D21), 8127, doi:10.1029/2001JD000514, 2002b.
- 1223 Noble, C. A., and K. A. Prather, Real-time measurement of correlated size
1224 and composition profiles of individual atmospheric aerosol particles,
1225 *Environ. Sci. Technol.*, 30, 2667–2680, 1996.
- 1226 Novakov, T., M. O. Andreae, R. Gabriel, T. W. Kirchstetter, O. L. Mayol-
1227 Bracero, and V. Ramanathan, Origin of carbonaceous aerosols over the
1228 tropical Indian Ocean: Biomass burning or fossil fuels?, *Geophys. Res.*
1229 *Let.*, 27(24), 4061–4064, 2000.
- 1230 Parsons, R. L., and R. R. Dickerson, NOAA ship Ronald H. Brown: Study
1231 global climate variability, *Sea Technol.*, 40(6), 39–45, 1999.
- 1232 Penner, J. E., R. E. Dickinson, and C. A. O'Neill, Effects of aerosol from
1233 biomass burning on the global radiation budget, *Science*, 256(5062),
1234 1432–1434, 1992.
- 1235 Penner, J. E., H. Eddleman, and T. Novakov, Towards the development of a
1236 global inventory for black carbon emissions, *Atmos. Environ., Part A*,
1237 27(8), 1277–1295, 1993.
- 1238 Podgorny, I. A., W. Conant, V. Ramanathan, and S. K. Satheesh, Aerosol
1239 modulation of atmospheric and surface solar heating over the tropical
1240 Indian Ocean, *Tellus, Ser. B*, 52(3), 947–958, 2000.
- 1241 Prather, K. A., T. Nordmeyer, and K. Salt, Real-time characterization of
1242 individual aerosol particles using time-of-flight mass spectrometry, *Anal.*
1243 *Chem.*, 66(9), 1403–1407, 1994.
- 1244 Pszenny, A. A. P., Particle size distributions of methanesulfonate in the
1245 tropical Pacific marine boundary layer, *J. Atmos. Chem.*, 14(1–4),
1246 273–284, 1992.
- 1247 Quinn, P. K., D. J. Coffman, V. N. Kapustin, T. S. Bates, and D. S. Covert,
1248 Aerosol optical properties in the marine boundary layer during the First
1249 Aerosol Characterization Experiment (ACE 1) and the underlying chemi-
1250 cal and physical aerosol properties, *J. Geophys. Res.*, 103(D13),
1251 16,547–16,563, 1998.
- 1252 Quinn, P. K., D. J. Coffmann, T. S. Bates, T. L. Miller, J. E. Johnson,
1253 K. Voss, E. J. Welton, C. Neusüß, P. Miller, and J. Sheridan, Aerosol optical
1254 properties during INDOEX 99: Means, variability, and controlling fac-
1255 tors, *J. Geophys. Res.*, 107(D9), 8020, doi:10.1029/2000JD000037, 2002.
- Ramanathan, V., et al., Indian Ocean Experiment (INDOEX) White Paper,
C⁴, Scripps Inst. of Oceanogr., La Jolla, Calif., 1995. 1256
1257
- Ramanathan, V., et al., Indian Ocean Experiment (INDOEX), A multi-
agency proposal for field experiment in the Indian Ocean, C⁴ publ. 1258
162, 83 pp., Scripps Inst. of Oceanogr., La Jolla, Calif., 1996. 1259
1260
- Ramanathan, V., et al., The Indian Ocean Experiment: Widespread haze
from south and southeast Asia and its climate forcing, *J. Geophys. Res.*,
106, 28,371–28,398, 2001. 1261
1262
- Rasch, P. J., W. D. Collins, and B. E. Eaton, Understanding the Indian
Ocean Experiment (INDOEX) aerosol distributions with an aerosol as-
similation, *J. Geophys. Res.*, 106(D7), 7337–7355, 2001. 1263
1264
- Ravindranath, N. H., and D. O. Hall, *Biomass, Energy and Environment: A*
Developing Country Perspective From India, Oxford Univ. Press, New
York, 1995. 1265
1266
- Reddy, M. S., and C. Venkataraman, Atmospheric optical and radiative
effects of anthropogenic aerosol constituents from India, *Atmos. Environ.*,
34(26), 4511–4523, 2000. 1267
1272
- Reddy, M. S., and C. Venkataraman, Inventory of aerosol and sulphur
dioxide emissions from India: Part Fossil fuel combustion, I., *Atmos.*
Environ., 36(4), 677–697, 2001a. 1273
1274
- Reddy, M. S., and C. Venkataraman, Inventory of aerosol and sulphur di-
oxide emissions from India: Part II. Biomass combustion, *Atmos. Environ.*,
36(4), 699–712, 2001b. 1275
1276
- Reid, J. S., P. V. Hobbs, C. Liousse, J. V. Martins, R. E. Weiss, and T. F.
Eck, Comparisons of techniques for measuring shortwave absorption and
black carbon content of aerosols from biomass burning in Brazil,
J. Geophys. Res., 103(D24), 32,031–32,040, 1998. 1277
1282
- Reiner, T., D. Sprung, C. Jost, R. Gabriel, O. L. Mayol-Bracero, M. O.
Andreae, T. L. Campos, and R. E. Shetter, Chemical characterization of
pollution layers over the tropical Indian Ocean: Signature of emissions
from biomass and fossil fuel burning, *J. Geophys. Res.*, 106(D22),
28,497–28,510, 2001. 1283
1284
- Rosenfeld, D., Suppression of rain and snow by urban and industrial air
pollution, *Science*, 287(5459), 1793–1796, 2000. 1285
1289
- Ruellan, S., H. Cachier, A. Gaudichet, P. Masclet, and J. P. Lacaux, Air-
borne aerosols over central Africa during the experiment for regional
sources and sinks of oxidants (EXPRESSO), *J. Geophys. Res.*, 104,
30,673–30,690, 1999. 1290
1291
- Satheesh, S. K., V. Ramanathan, L. J. Xu, J. M. Lobert, I. A. Podgorny,
J. M. Prospero, B. N. Holben, and N. G. Loeb, A model for the natural
and anthropogenic aerosols over the tropical Indian Ocean derived from
Indian Ocean Experiment data, *J. Geophys. Res.*, 104(D22), 27,421–
27,440, 1999. 1292
1293
- Schmid, H., et al., Results of the “Carbon Conference” international carbon
round robin test stage I, *Atmos. Environ.*, 35(12), 2111–2121, 2001. 1294
1300
- Schwartz, S. E., and M. O. Andreae, Uncertainty in climate change caused
by aerosols, *Science*, 272(5265), 1121–1122, 1996. 1301
1302
- Schwartz, S. E., The white house effect: Shortwave radiative forcing of
climate by anthropogenic aerosols: An overview, *J. Aerosol Sci.*, 27(3),
359–382, 1996. 1303
1304
- Shah, J. J., and J. A. Rau, Carbonaceous species methods comparison
study: Interlaboratory round robin interpretation of results, Res. Div.,
Calif. Air Res. Board, *Final Rep. G2E-0024*, Sacramento, Calif.,
1991. 1305
1309
- Silva, P. J., and K. A. Prather, On-line characterization of individual parti-
cles from automobile emissions, *Environ. Sci. Technol.*, 31(11), 3074–
3080, 1997. 1310
1311
- Silva, P. J., D.-Y. Liu, C. A. Noble, and K. A. Prather, Size and chemical
characterization of individual particles resulting from biomass burning of
local Southern California species, *Environ. Sci. Technol.*, 33(18), 3068–
3076, 1999. 1312
1316
- Smith, D. J. T., R. M. Harrison, L. Luhana, C. A. Pio, L. M. Castro, M. N.
Tariq, S. Hayat, and T. Quraishi, Concentrations of particulate airborne
polycyclic aromatic hydrocarbons and metals collected in Lahore, Paki-
stan, *Atmos. Environ.*, 30(23), 4031–4040, 1996. 1313
1319
- Smith, K. R., R. Uma, V. V. N. Kishore, K. Lata, V. Joshi, J. Zhang, R. A.
Rasmussen, and M. A. K. Khalil, Greenhouse gases from small-scale
combustion devices in developing countries: Phase I Household stoves
in India, I., *EPA-600/R-00-052*, Office of Res. and Dev., U.S. Environ.
Protect. Agency, Washington, D.C., 2000. 1320
1321
- Sprung, D., C. Jost, T. Reiner, A. Hansel, and A. Wisthaler, Acetone
and acetonitrile in the tropical Indian Ocean boundary layer and
free troposphere: Aircraft-based intercomparison of AP-CIMS and
PTR-MS measurements, *J. Geophys. Res.*, 106, 28,511–28,527,
2001. 1322
1327
- Stehr, J. W., W. P. Ball, R. R. Dickerson, B. G. Doddridge, C. Piety, and
J. E. Johnson, Latitudinal gradients in O₃ and CO during INDOEX 1999,
J. Geophys. Res., 107(D19), 8016, doi:10.1029/2001JD000446, 2002. 1328
1329
- Stevens, R. K., T. G. Dzubay, R. W. Shaw Jr., W. A. McClenny, C. W.
Lewis, and W. E. Wilson, *Science*, 14, 1491, 1980. 1330
1331
1332
1333
1334
1335

- 1336 Streets, D. G., and S. T. Waldhoff, Greenhouse-gas emissions from biofuel
 1337 combustion in Asia, *Energy*, 24, 841–855, 1999.
- 1338 Streets, D. G., S. K. Guttikunda, and G. R. Carmichael, The growing
 1339 contribution of sulfur emissions from ships in Asian waters, 1988–
 1340 1995, *Atmos. Environ.*, 34, 4425–4439, 2000.
- 1341 Thornton, D. C., A. R. Bandy, B. W. Blomquist, A. R. Driedger, and T. P.
 1342 Wade, Sulfur dioxide contribution over the Pacific Ocean 1991–1996,
 1343 *J. Geophys. Res.*, 104, 5845–5854, 1999.
- 1344 Turpin, B. J., J. J. Huntzicker, and S. V. Hering, Investigaton of organic
 1345 aerosol sampling artifacts in the Los Angeles Basin, *Atmos. Environ.*, 28,
 1346 3061–3071, 1994.
- 1347 Twomey, S., *Atmospheric Aerosols*, 302 pp., Elsevier, New York 1997.
- 1348 United Nations Environmental Program (UNEP), Environmental impacts of
 1349 trade liberalization and polices for sustainable management of natural
 1350 resources: A case study on India's automobile sector, *UNEP/99/2*, 177
 1351 pp., United Nations Environ. Programme, Nairobi, 1999.
- 1352 United Nations Environmental Program (UNEP), Assessment Report,
 1353 Asian brown cloud: Climate and other environmental impacts, UNEP
 1354 and C4, United Nations Environ. Programme, Nairobi, 2002.
- 1355 Verver, G. H. L., D. R. Sikka, J. M. Lobert, G. Stossmeister, and
 1356 M. Zachariasse, Overview of the meteorological conditions and atmo-
 1357 spheric transport processes during INDOEX 1999, *J. Geophys. Res.*,
 1358 106, 28,399–28,413, 2001.
- 1359 Wang, H.-C., and W. John, Characteristics of the Berner impactor for
 1360 sampling inorganic ions, *Aerosol Sci. Technol.*, 8, 157–172, 1988.
- 1361 Welton, E. J., K. J. Voss, P. K. Quinn, P. J. Flatau, K. Markowicz, J. R.
 1362 Campbell, J. D. Spinhirne, H. R. Gordon, and J. E. Johnson, Measure-
 1363 ments of aerosol vertical profiles and optical properties during INDOEX
 1364 1999 using micro-pulse lidars, *J. Geophys. Res.*, 107(D9), 8019,
 1365 doi:10.1029/2000JD000038, 2002.
- 1366 Wenzel, R. J., D.-Y. Liu, E. S. Edgerton, and K. A. Prather, Aerosol time-
 1367 of-flight mass spectrometry during the Atlanta Supersite Experiment: 2.
 1368 Scaling procedures, *J. Geophys. Res.*, 108(D7), 8427, doi:10.1029/
 1369 2001JD001563, 2003.
- 1370 Winchester, J. W., and G. D. Nifong, Water pollution in Lake Michigan by
 1371 trace elements from pollution aerosol fallout, *Water Air Soil Pollut.*, 1,
 1372 50–64, 1971.
- Wisthaler, A., A. Hansel, P. Crutzen, and R. Dickerson, Organic trace gas
 measurements by PTR-MS during INDOEX 1999, *J. Geophys. Res.*,
 107(D19), 8024, doi:10.1029/2001JD000576, 2002.
- Yamasoe, M. A., A. Paulo, A. H. Miguel, and A. G. Allen, Chemical
 composition of aerosol particles from different emissions of vegetation
 fires in the Amazon Basin: Water-soluble species and trace elements,
Atmos. Environ., 34, 1641–1653, 2000.
- W. P. Ball, Department of Chemistry, University of Maryland, College
 Park, MD 20742, USA. (ball@metosrv2.umd.edu)
- T. S. Bates and P. K. Quinn, NOAA, Pacific Marine Environmental
 Laboratory, 7600 Sand Point Way, NE, Seattle, WA 98115, USA.
 (bates@pmel.noaa.gov; quinn@pmel.noaa.gov)
- K. R. Coffee, Lawrence Livermore National Laboratory, 7000 East Ave
 L-231, Livermore, CA 94550, USA. (coffee3@llnl.gov)
- P. J. Crutzen, Atmospheric Chemistry Division, Max-Planck Institute for
 Chemistry, J.J. Becher-weg 27, D-55128 Mainz, Germany. (aira@mpch-
 mainz.mpg.de)
- R. R. Dickerson, Department of Meteorology and Department of
 Chemistry, University of Maryland, College Park, MD 20742, USA.
 (russ@atmos.umd.edu)
- S. A. Guazzotti, Department of Chemistry and Biochemistry, University
 of California, San Diego, CA 92037, USA. (serad@chem.ucsd.edu)
- A. Hansel and A. Wisthaler, Institut für Ionenphysik, University of
 Innsbruck, Technikerstrasse 25, A-6020, Innsbruck, Austria. (Armin.
 Hansel@uibk.ac.at; Armin.Wisthaler@uibk.ac.at)
- C. Neusüß, Institut für Troposphärenforschung, Permoserstrasse 15,
 D-04303 Leipzig, Germany. (CNE@bsax.de)
- K. A. Prather, Department of Chemistry and Biochemistry, University of
 California, San Diego, 9500 Gilman Drive, La Jolla, CA 92093, USA.
 (kprather@chem.ucsd.edu)
- D. T. Suess, Department of Chemistry, University of California,
 Riverside, CA 92521, USA. (dtsuess@citrus.ucr.edu)

Article